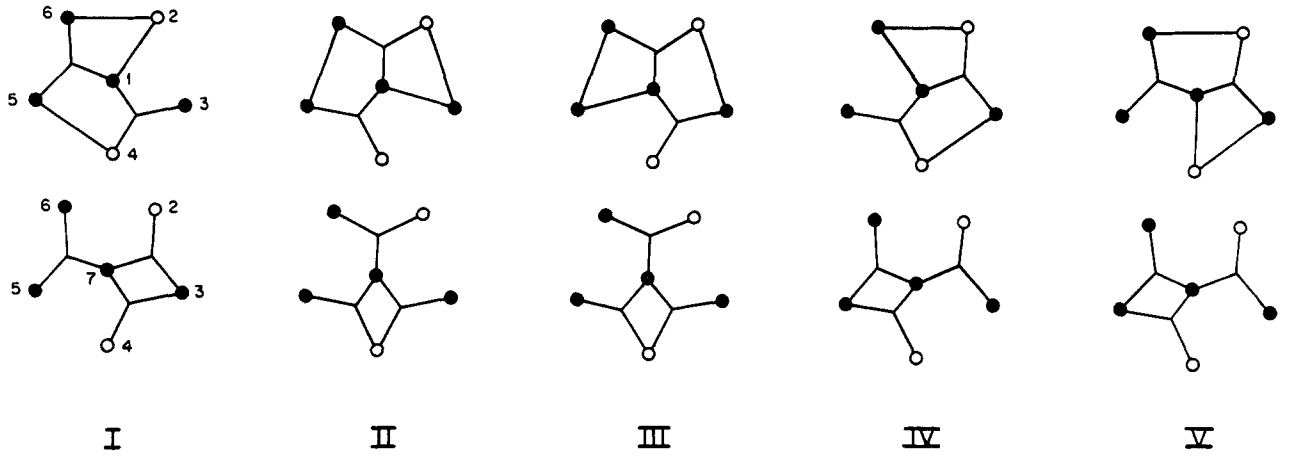

Figure 9. Topologically allowed structures for 2,4-$C_2B_5H_7$. The dots are boron and the circles are carbon, and the two pentagonal pyramids are shown separately for clarity. Each of these structures has three other symmetry equivalent structures.

Table XIII. Population Analysis for Topologically Allowed Structures I and V

	I	V
	Charges	
B_1	−0.167	−0.167
B_3	0.0	−0.333
B_5	−0.167	−0.167
	Overlap Populations	
B_1–B_3	0.500	0.667
B_1–B_5	0.667	0.833
B_5–B_6	1.334	1.334
C_2–B_6	1.000	0.833
C_2–B_3	1.000	1.000

describing 2,4-$C_2B_5H_7$ assuming, of course, that a proper weighting scheme can be developed which is independent of SCF and LMO calculations.

The use of fractional bonds in 2,4-$C_2B_5H_7$ and 4,5-$C_2B_4H_8$ allows us to write single valence structures which describe the bonding more accurately than any single topologically allowed structure. For the more symmetrical 1,6-$C_2B_4H_6$ and B_5H_9 the fractional bonding arrangements presented here allow us to write a set of symmetry equivalent structures which describe the bonding as well as or better than the corresponding, sometimes larger, set of topologically allowed structures.

Acknowledgments. We wish to acknowledge support of this research by the Office of Naval Research and the National Institutes of Health, and we thank the National Science Foundation for the award of a Predoctoral Fellowship to D. S. M. We also thank Dr. Richard M. Stevens for use of his polyatomic SCF program.

A Self-Consistent Field and Localized Orbital Study of 4,5-Dicarbahexaborane(8)

Dennis S. Marynick and William N. Lipscomb*

Contribution from the Department of Chemistry, Harvard University, Cambridge, Massachusetts 02138. *Received June 1, 1972*

Abstract: A self-consistent field wave function has been calculated for 4,5-dicarbahexaborane(8) using the experimental geometry and a minimum basis set of Slater orbitals. The charge distribution, reactivity, diamagnetic chemical shifts, ionization potential, atomization energies, and dipole moments are discussed in terms of the ground-state charge distribution. Localized orbitals are found by the Edmiston–Ruedenberg method and a modified Taylor method, and the valence structure of the molecule is described in terms of fractional three-center bonds. A detailed discussion of the nature of the extremum in the self-repulsion energy surface is presented. The relationship between the topological theory of the boron hydrides and the valence structure of the molecule is discussed.

Dicarbahexaborane(8) (4,5-$C_2B_4H_8$) is a member of the carborane series with the general formula $C_nB_{6-n}H_{10-n}$ (n = 1, 2, 3, or 4) and may be considered to be derived from hexaborane(10) by replacement of two BH units (B_4–H_b and B_3–H_b) with carbon. First discovered by Weiss and Shapiro,[1] this compound was characterized structurally by its ^{11}B nmr spectrum[2,3] and by a single-crystal X-ray diffraction study[4]

(1) H. G. Weiss and I. Shapiro, U. S. Patent 3,086,996 (April 1963).

(2) T. P. Onak, R. E. Williams, and H. G. Weiss, *J. Amer. Chem. Soc.*, **84**, 2830 (1962).

(3) R. E. Williams and T. P. Onak, *ibid.*, 86, 3159 (1964).

(4) W. E. Streib, F. P. Boer, and W. N. Lipscomb, *ibid.*, **85**, 2331 (1963); F. P. Boer, W. E. Streib, and W. N. Lipscomb, *Inorg. Chem.*, 3, 1666 (1964).

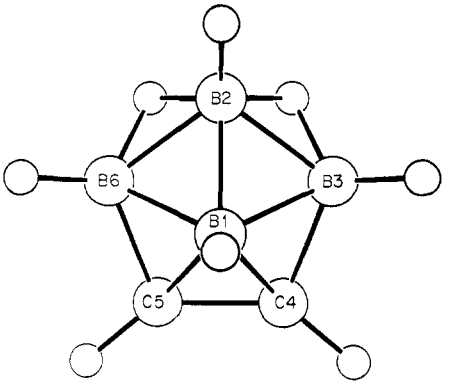

Figure 1. 4,5-Dicarbahexaborane(8).

of the parent compound and the *C,C'*-dimethyl derivative. In addition to being an important precursor to several smaller carboranes, $C_2B_4H_8$ has been the subject of a number of chemical studies which have resulted in the preparation of the *B*-deuterio,[5] *B*-chloro,[6] *B*-bromo,[6] *B*-methyl,[7] and several *C*-alkyl derivatives.[2]

The valence structure of $C_2B_4H_8$ is very interesting for several reasons. First, on the basis of bond distances and angles Boer, Streib, and Lipscomb proposed[4] that the two carbons make up an ethylenic system with π donation to the apex boron. Our localized molecular orbital (LMO) calculations provide a method of testing this hypothesis. Second, if we consider $C_2B_4H_8$ to be equivalent to $B_6H_8^{2-}$ and treat the molecule topologically, we find[8] that there are no topologically allowed structures and therefore the topological theory of the boron hydrides in its present form is not applicable to this compound. Finally, as mentioned above, $C_2B_4H_8$ is a member of the isoelectronic and isostructural series B_6H_{10}, CB_5H_9, $C_2B_4H_8$, $C_3B_5H_7$, and $C_4B_2H_6$, and when accurate molecular geometries become available for all of these compounds we expect to have a unique opportunity to study in detail the effects of carbon for B–H substitution on molecular properties and valence structure in a closely related series of molecules. This comparison may be especially important in correlating the chemistry of the boron hydrides and carboranes.

In this paper we present the SCF wave function for $C_2B_4H_8$ and we examine a number of molecular properties including charge distribution, overlap populations, bond midpoint densities, ionization potentials, diamagnetic chemical shifts, dipole moments, and atomization energies. We obtain LMO's from the SCF wave function by maximizing the self-repulsion energy[9a-d] using both the Edmiston–Ruedenberg[9e] (ER) and a modified Taylor[9f] (MT) method. The LMO's are discussed in terms of fractional bonding, per cent delocalization, and hybridization. We also include a discussion of the necessary modification of the topological theory of the boron hydride to describe correctly the bonding in this molecule. Finally, a preliminary comparison is made of the ER and MT methods of obtaining LMO's.

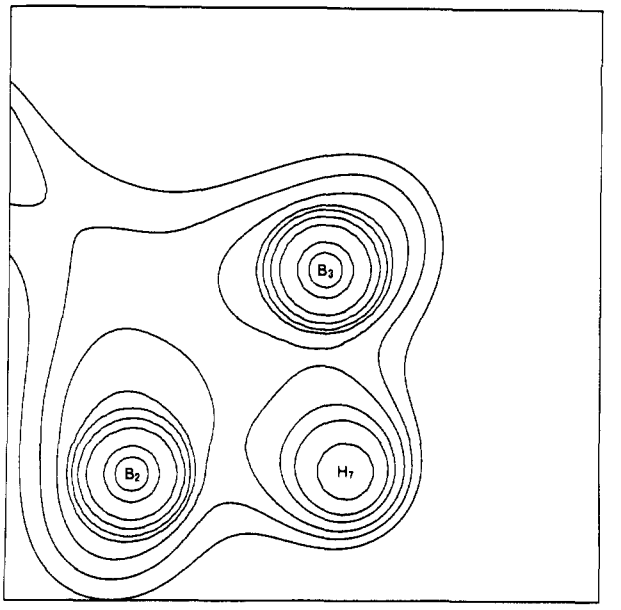

Figure 2. Electron density map of the $B_2H_7B_3$ plane. The contours in this map and all of the maps in this paper are 10.0, 3.0, 0.50, 0.25, 0.17, 0.14, 0.11, 0.09, and 0.07 e/au^3.

Procedure

The SCF calculation was performed with the use of Stevens' program[10] for the IBM 360/65. The geometry of $C_2B_4H_8$ (Figure 1) was taken from the X-ray diffraction study,[4] and the basis set used (Table I) was the same as that given in the previous paper. The coordinates and wave function are listed in Tables II and III.

Table I. Exponents

B	1s	4.68	C	1s	5.680	$B-H_t$	1.147
	2s	1.443		2s	1.730	$B-H_b$	1.209
	2p	1.477		2p	1.760	C–H	1.160

Table II. Coordinates of Unique Atoms[a]

	x	*y*	*z*
B_1	2.4947	0.0	2.0386
B_2	0.0	0.0	0.0
B_3	2.1568	2.5753	−0.0607
C_4	4.7547	1.3525	0.0
H_1	2.5834	0.0	4.2667
H_2	−2.1730	0.0	0.2362
H_3	1.8430	4.7326	0.4083
H_4	6.4240	2.4100	0.5897
H_7	0.6610	1.7115	−1.8275

[a] Atomic units; the symmetry plane is *xz*.

The program for localizing molecular orbitals by the ER method has been previously described.[11] One of us

(5) J. R. Spielman, R. Warren, G. B. Dunks, J. E. Scott, and T. Onak, *Inorg. Chem.*, 7, 216 (1968); T. Onak and G. B. Dunks, *ibid.*, **5**, 439 (1966).
(6) J. R. Spielman, G. B. Dunks, and R. Warren, *ibid.*, **8**, 2172 (1969).
(7) T. Onak, D. Marynick, P. Mattschei, and G. Dunks, *ibid.*, 7, 1754 (1968).
(8) I. R. Epstein and W. N. Lipscomb, *ibid.*, **10**, 1921 (1971).
(9) (a) J. C. Lennard-Jones, *Proc. Roy. Soc., Ser. A*, **198**, 1, 14 (1949); (b) G. G. Hall and J. E. Lennard-Jones, *ibid.*, **202**, 155 (1950); (c) J. E. Lennard-Jones and J. A. Pople, *ibid.*, **202**, 166 (1950); (d) *ibid.*, **210**, 190 (1951); (e) C. Edmiston and K. Ruedenberg, *Rev. Mod. Phys.*, **35**, 467 (1963); (f) W. J. Taylor, *J. Chem. Phys.*, **48**, 2385 (1968).
(10) R. M. Stevens, *ibid.*, **52**, 1397 (1970).
(11) (a) E. Switkes, R. M. Stevens, W. N. Lipscomb, and M. D. Newton, *ibid.*, **51**, 2085 (1969); (b) E. Switkes, W. N. Lipscomb, and M. D. Newton, *J. Amer. Chem. Soc.*, **92**, 3847 (1970); (c) I. R. Epstein, J. A. Tossell, E. Switkes, R. M. Stevens, and W. N. Lipscomb, *Inorg. Chem.*, **10**, 171 (1971).

Table III. $C_2B_4H_8$ Occupied Orbitals and Eigenvalues

	1 A' -11.2375	2 A'' -11.2370	3 A' -7.6179	4 A'' -7.5622	5 A' -7.5621	6 A' -7.5596	7 A' -1.1165	8 A' -0.8839	9 A'' -0.8435	10 A' -0.6913	11 A'' -0.6752	12 A' -0.6334	13 A' -0.6065	14 A' -0.5231	15 A'' -0.4988	16 A'' -0.4950	17 A'' -0.4874	18 A' -0.4594	19 A'' -0.4126	20 A'' -0.3467
B1-1S	-0.0003	0.0000	-0.0040	0.0000	-0.0689	-0.9914	0.0877	-0.0525	0.0000	-0.1121	0.0000	-0.1072	-0.0631	0.0381	0.0000	0.0232	0.0000	0.0138	0.0077	0.0000
B1-2S	0.0029	0.0000	0.0034	0.0000	0.0033	-0.0299	-0.1477	0.1020	0.0000	0.3013	0.0000	0.3082	0.1889	-0.0888	0.0000	-0.0706	0.0000	-0.0253	0.0319	0.0000
B1-2PZ	-0.0013	0.0000	-0.0012	0.0000	-0.0015	0.0051	0.0960	-0.0670	0.0000	-0.0719	0.0000	0.1319	0.0420	-0.0041	0.0000	-0.2742	0.0000	-0.2891	-0.1596	0.0000
B1-2PX	0.0024	0.0000	-0.0024	0.0000	-0.0001	0.0001	-0.0351	-0.0910	0.0000	0.0355	0.0000	-0.0391	-0.0086	0.0804	0.0000	-0.1141	0.0000	-0.1582	0.3563	0.0000
B1-2PY	0.0000	-0.0011	0.0000	0.0038	0.0000	0.0000	0.0000	0.0000	-0.1146	0.0000	0.0420	0.0000	0.0000	0.0000	0.1831	0.0000	0.0267	0.0000	0.0000	0.4086
B2-1S	-0.0000	0.0000	-0.9940	0.0000	0.0036	0.0036	0.0475	-0.1457	0.0000	0.0705	0.0000	-0.0242	-0.0902	-0.0210	0.0000	-0.0554	0.0000	-0.0250	0.0166	0.0000
B2-2S	-0.0002	0.0000	-0.0291	0.0000	0.0046	0.0038	-0.0795	0.3281	0.0000	-0.1950	0.0000	0.0736	0.2587	0.0498	0.0000	0.1567	0.0000	0.0828	-0.0616	0.0000
B2-2PZ	0.0001	0.0000	0.0015	0.0000	0.0006	0.0023	-0.0022	-0.0334	0.0000	0.1329	0.0000	0.1310	0.0596	0.0513	0.0000	0.1486	0.0000	0.2102	-0.2288	0.0000
B2-2PX	-0.0004	0.0000	-0.0034	0.0000	0.0024	0.0018	-0.0557	0.1112	0.0000	0.1086	0.0000	-0.0363	-0.1219	-0.1442	0.0000	-0.0333	0.0000	0.1698	-0.0796	0.0000
B2-2PY	0.0000	0.0001	0.0000	0.0031	0.0000	0.0000	0.0000	0.0001	-0.0756	0.0000	0.2182	0.0000	0.0000	0.0000	-0.1498	0.0000	0.1779	0.0000	0.0000	0.1836
B3-1S	-0.0002	0.0002	-0.0026	-0.7028	-0.7012	0.0684	0.0655	-0.0711	0.1067	-0.0038	-0.0939	-0.0243	0.0902	-0.0261	-0.0259	0.0156	0.0306	-0.0196	0.0078	0.0083
B3-2S	0.0029	-0.0031	0.0027	-0.0206	-0.0200	0.0052	-0.1059	0.1401	-0.2465	0.0014	0.2405	0.0658	-0.2535	0.0851	0.0855	-0.0469	-0.0831	0.0431	-0.0535	-0.0384
B3-2PZ	-0.0002	0.0001	0.0004	-0.0003	-0.0003	0.0022	-0.0074	-0.0108	-0.0050	0.0903	-0.0312	0.1177	0.0395	0.0267	0.0996	0.0527	-0.1089	0.1386	0.0409	0.3393
B3-2PX	0.0022	-0.0022	-0.0016	0.0003	0.0004	0.0004	-0.0359	-0.0732	-0.0713	0.0746	-0.1226	-0.0168	-0.1021	0.0882	0.2312	0.1242	-0.0077	-0.1772	-0.0302	-0.1783
B3-2PY	-0.0007	0.0010	-0.0019	0.0028	0.0025	-0.0020	0.0649	-0.0737	0.0580	-0.0611	-0.0239	0.0819	-0.0908	0.1476	-0.1117	-0.1700	-0.3172	0.1010	0.0257	-0.0981
C4-1S	-0.7037	0.7034	-0.0000	0.0001	0.0000	-0.0001	0.1422	0.0772	0.1213	0.0301	0.0427	0.0206	0.0052	-0.0182	-0.0147	-0.0037	-0.0232	0.0119	0.0248	0.0259
C4-2S	-0.0147	0.0202	-0.0000	0.0030	0.0031	0.0020	-0.3786	-0.2457	-0.3814	-0.1131	-0.2094	-0.0810	-0.0213	0.0803	0.0621	-0.0049	0.0844	-0.0504	-0.1154	-0.1135
C4-2PZ	-0.0015	0.0011	-0.0001	-0.0004	-0.0005	0.0016	-0.0327	-0.0253	-0.0329	0.0468	-0.0435	0.1603	0.0778	-0.0579	-0.0230	0.0177	-0.0139	0.0573	0.4576	0.2468
C4-2PX	0.0010	-0.0006	0.0000	-0.0014	-0.0015	-0.0009	0.0602	-0.0984	0.0509	-0.2530	-0.1349	0.1190	0.1182	-0.1729	-0.3494	-0.0518	-0.0304	0.1605	-0.0635	0.1137
C4-2PY	-0.0013	-0.0028	0.0000	0.0009	0.0008	-0.0009	0.1008	0.0761	-0.1389	-0.0576	-0.0917	0.2326	-0.2626	-0.0632	-0.0113	0.2820	0.0020	-0.2085	0.0156	-0.0819
C5-1S	-0.7037	-0.7034	-0.0000	-0.0001	0.0000	-0.0001	0.1422	0.0772	-0.1213	0.0301	-0.0427	0.0206	0.0052	-0.0182	0.0147	-0.0037	0.0232	0.0119	0.0248	-0.0259
C5-2S	-0.0147	-0.0202	-0.0000	-0.0030	0.0031	0.0020	-0.3786	-0.2457	0.3814	-0.1131	0.2094	-0.0810	-0.0213	0.0803	-0.0621	-0.0049	-0.0844	-0.0504	-0.1154	0.1135
C5-2PZ	-0.0015	-0.0011	-0.0001	0.0004	-0.0005	0.0016	-0.0327	-0.0253	0.0329	0.0468	0.0435	0.1603	0.0778	-0.0579	0.0230	0.0177	0.0139	0.0573	0.4576	-0.2468
C5-2PX	0.0010	0.0006	0.0000	0.0014	-0.0015	-0.0009	0.0602	-0.0984	-0.0509	-0.2530	0.1349	0.1190	0.1182	-0.1729	0.3494	-0.0518	0.0304	0.1605	-0.0635	-0.1137
C5-2PY	0.0013	-0.0028	0.0000	0.0009	-0.0008	0.0009	-0.1008	-0.0761	-0.1389	0.0576	-0.0917	-0.2326	0.2626	0.0632	-0.0113	-0.2820	0.0020	0.2085	-0.0156	-0.0819
B6-1S	-0.0002	-0.0002	-0.0026	0.7028	-0.7012	0.0684	0.0655	-0.0711	-0.1067	-0.0038	0.0939	-0.0243	0.0902	-0.0261	0.0259	0.0156	-0.0306	-0.0196	0.0078	-0.0083
B6-2S	0.0029	0.0031	0.0027	0.0206	-0.0200	0.0052	-0.1059	0.1401	0.2465	0.0014	-0.2405	0.0658	-0.2535	0.0851	-0.0855	-0.0469	0.0831	0.0431	-0.0535	0.0384
B6-2PZ	-0.0002	-0.0001	0.0004	0.0003	-0.0003	0.0022	-0.0074	-0.0108	0.0050	0.0903	0.0312	0.1177	0.0395	0.0267	-0.0996	0.0527	0.1089	0.1386	0.0409	-0.3393
B6-2PX	0.0022	0.0022	-0.0016	-0.0003	0.0004	0.0004	-0.0359	-0.0732	0.0713	0.0746	0.1226	-0.0168	-0.1021	0.0882	-0.2312	0.1242	0.0077	-0.1772	-0.0302	0.1783
B6-2PY	0.0007	0.0010	0.0019	0.0028	-0.0025	0.0020	-0.0649	0.0737	0.0580	0.0611	-0.0239	-0.0819	0.0908	-0.1476	-0.1117	0.1700	-0.3172	-0.1010	-0.0257	-0.0981
H1-1S	-0.0002	0.0000	-0.0000	0.0000	0.0001	0.0042	-0.0258	0.0201	0.0000	0.1107	0.0000	0.2508	0.1328	-0.0723	0.0000	-0.3121	0.0000	-0.3408	-0.2370	0.0000
H2-1S	-0.0001	0.0000	0.0045	0.0000	0.0001	-0.0001	-0.0130	0.0873	0.0000	-0.1507	0.0000	0.0791	0.2554	0.4366	0.0000	0.1880	0.0000	-0.0880	-0.0009	0.0000
H3-1S	-0.0002	0.0001	0.0001	0.0032	-0.0003	-0.0172	0.0352	-0.0726	-0.0271	0.1211	0.1090	-0.1939	0.1770	-0.0634	-0.2046	-0.3988	0.2131	0.0053	-0.0300	
H4-1S	0.0033	-0.0034	0.0000	0.0002	0.0003	0.0002	-0.0641	-0.1084	-0.1647	-0.2158	-0.2346	0.1787	-0.0350	-0.1547	-0.2976	0.1340	0.0203	0.0055	0.0153	0.0979
H5-1S	0.0033	0.0034	0.0000	-0.0002	0.0003	0.0002	-0.0641	-0.1084	0.1647	-0.2158	0.2346	0.1787	-0.0350	-0.1547	0.2976	0.1340	-0.0203	0.0055	0.0153	-0.0979
H6-1S	-0.0002	-0.0001	0.0001	-0.0032	0.0032	-0.0003	-0.0172	0.0352	0.0726	-0.0271	-0.1211	0.1090	-0.1939	0.1770	0.0634	-0.2046	0.3988	0.2131	0.0053	0.0300
H7-1S	-0.0001	0.0001	0.0039	0.0030	0.0030	-0.0004	-0.0414	0.1786	-0.0834	-0.1936	0.2453	-0.0977	-0.0309	-0.1136	0.2220	-0.1549	0.2080	-0.1383	0.1383	-0.1325
H8-1S	-0.0001	-0.0001	0.0039	-0.0030	0.0030	-0.0004	-0.0414	0.1786	0.0834	-0.1936	-0.2453	-0.0977	-0.0309	-0.1136	0.2220	-0.1549	-0.2080	-0.1383	0.1383	0.1325

Table IV. Energetics[a]

Kinetic energy	179.236
Nuclear attraction energy	−786.394
Two electron energy	242.129
Nuclear repulsion energy	186.279
Total energy	−178.744
$-E/T$	0.997
Ionization potential	0.347
Atomization energy[b]	−1.5107 (948 kcal)
Atomization energy[c]	−2.4339 (1527 kcal)

[a] Atomic units. [b] Best single exponent: see E. Clementi and D. L. Raimondi, *J. Chem. Phys.*, **38**, 2686 (1963). [c] Reference atoms employ molecular exponents.

Table V. Dipole Moments[a]

	z	Total
B_1	−0.28	0.28
B_2	−0.43	0.48
B_3	0.01	0.45
C_4	0.58	0.63
B_1–B_2	−0.20	0.31
B_1–B_3	−0.40	0.54
B_1–C_4	−0.46	0.51
B_2–B_3	−0.15	0.21
B_2–C_4	0.02	0.08
B_3–C_4	0.58	0.63
B_1–H_1	−1.27	1.27
B_2–H_2	−0.18	1.32
B_2–H_7	0.51	0.66
B_3–H_3	−0.25	1.30
B_3–H_7	0.63	0.76
C_4–H_4	0.33	1.09
Total atomic moment	0.48	0.48
Total bond moment	−1.00	1.19
Total ionic moment	−1.07	1.34
Total dipole moment	−1.60	2.11

[a] Debyes.

(D. S. M.) has now written in collaboration with J. H. Hall a program employing a modified Taylor method of localization. Computation times for the SCF and LMO calculations are comparable to those given in the previous paper.

Energetics and Dipole Moment

In Table IV we list the various components of the SCF energy, virial ratio, ionization potential, and atomization energies calculated as discussed in the previous paper. The dipole moment components are listed in Table V. No experimental results are available; however, we again note the remarkable consistency of both B–H and C–H bond moments. In agreement with earlier NEMO results,[12] the direction of the dipole moment makes the carbon end of the molecule positive, but in contrast to the boron hydrides that contain bridge hydrogens the net bond moment is in the same direction as the total dipole moment.

Population Analysis

We continue in this paper our practice of relying heavily on bond midpoint densities and electron density contour maps to describe the bonding. In Table VI we list the overlap populations, bond midpoint densities, and distances for all adjacent interactions. As in the previous paper, all three criteria predict the same relative bond strengths when restricted to bonds of the same type. Thus, the strongest B–B interaction is B_1–B_2, followed by B_1–B_3, and finally B_2–B_3, which is expected to be only weakly bonding because of the bridging hydrogen. The equatorial B_3–C_4 interaction is, as anticipated, considerably stronger than the apical B_1–C_4 bond. The bridge hydrogen asymmetry, which was considered to be experimentally significant and was included in the idealized coordinates of the molecule, is confirmed by both bond midpoint densities and overlap populations. The slight asymmetry is illustrated nicely in Figure 2. This result is in marked contrast[13] to that

Table VI. Overlap Populations and Electron Densities

Bond	Distance[a]	Overlap population	Midpoint density[b]
B_1–B_2	1.705	0.580	0.133
B_1–B_3	1.767	0.358	0.118
B_2–B_3	1.778	0.354	0.105
B_1–C_4	1.763	0.242	0.120
B_3–C_4	1.520	0.857	0.204
B_1–H_1	1.180	0.816	0.174
B_2–H_2	1.157	0.839	0.183
B_2–H_7	1.370	0.349	0.108
B_3–H_3	1.180	0.825	0.175
B_3–H_7	1.308	0.425	0.111

[a] Ångströms. [b] Electron/au^3.

(12) F. P. Boer, Ph.D. Thesis, 1965, University Microfilms 65–10, 683.

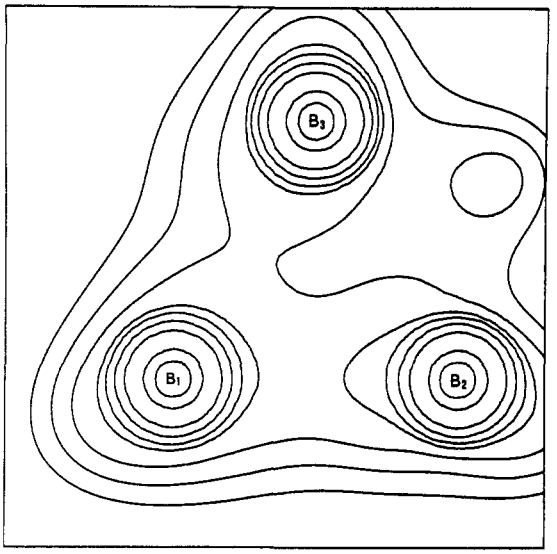

Figure 3. Electron density map of the $B_1B_2B_3$ plane.

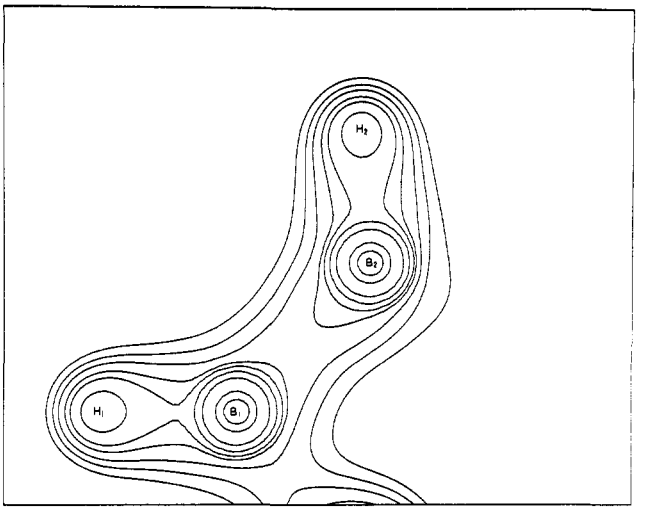

Figure 5. Electron density map of the $H_1B_1B_2H_2$ plane.

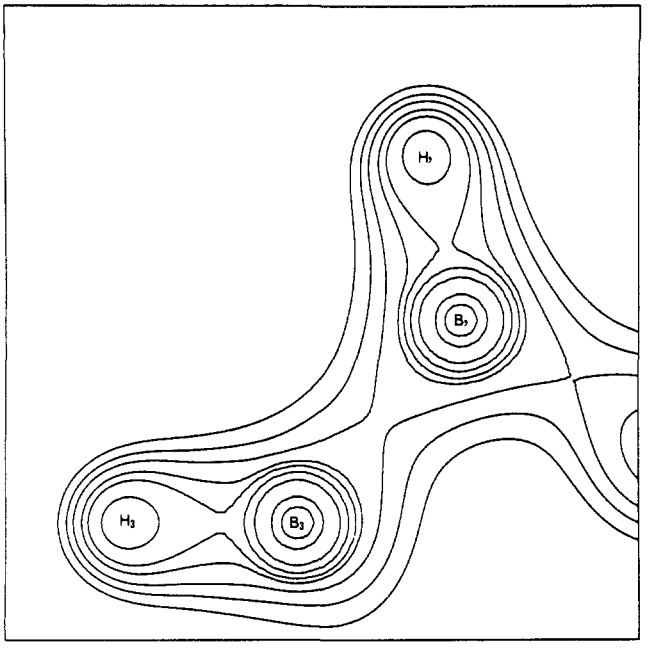

Figure 4. Electron density map of the $H_3B_3B_1$ plane.

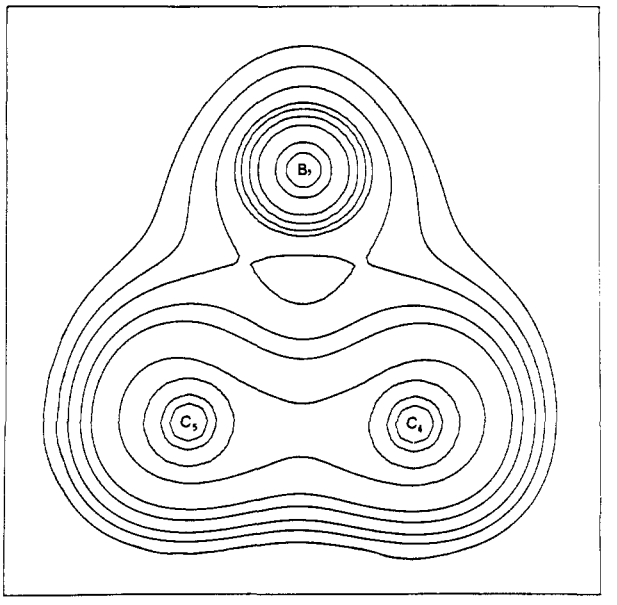

Figure 6. Electron density map of the $C_4C_5B_1$ plane.

for B_5H_{11}, where the bridge hydrogen not in the molecular plane of symmetry showed an asymmetric overlap population *opposite* to the very slight asymmetry implicit in the coordinates used.

The electron density in the $B_1B_2B_3$ plane (Figure 3) clearly illustrates the relative B–B bond strengths. Note especially the very weak direct B_2–B_3 interaction. Two other planes of interest are $H_3B_3B_1$ (Figure 4) and $H_1B_1B_2H_2$ (Figure 5). These maps give some idea of the relative B–H bond strengths, although B_1–H_1 in Figure 4 is out of the plane and may not be directly compared to the other B–H bonds. The overlap populations and bond midpoint densities indicate that the relative B–H bond strengths are B_2–H_2 > B_3–H_3 > B_1–H_1. The $C_4C_5B_1$ plane in Figure 6 shows strong B_1–C_1 and C_4–C_5 interactions which are very interesting when discussed in terms of LMO's (see below). The "hole" near the center of the $C_4C_5B_1$ triangle is a minimum in electron density.

The Mulliken charges and inner-shell eigenvalues[14] for each unique atom are given in Table VII. Both criteria predict that B_1 is the most negative boron,

Table VII. Mulliken Charges and Inner-Shell Eigenvalues

Atom	Charge	ϵ^a
B_1	0.020	−7.560
B_2	0.069	−7.618
B_3	0.061	−7.562
C_4	−0.016	−11.238
H_1	−0.084	
H_2	−0.051	
H_3	−0.083	
H_4	−0.083	
H_7	0.018	

[a] Atomic units.

(13) E. Switkes, I. R. Epstein, J. A. Tossell, R. M. Stevens, and W. N. Lipscomb, *J. Amer. Chem. Soc.*, **92**, 3837 (1970).

(14) R. J. Buenker and S. D. Peyerimhoff, *Chem. Phys. Lett.*, 3, 37 (1969).

followed by B_3 and B_2. A similar trend is found for the corresponding hydrogens. A further discussion of the charge distribution may be found in the section on reactivity.

Chemical Shifts

The ^1H absolute experimental chemical shifts, diamagnetic contributions with the gauge origin at the nucleus, and paramagnetic contributions calculated as in the previous paper are given in Table VIII. With

Table VIII. ^1H Chemical Shifts[a]

Atom	σ_{abs}[b]	σ_d	σ_p
H_1	31.4	176.5	−145.1
H_2	29.5	165.4	−135.9
H_3	29.5	167.5	−138.0
H_b	35.4	194.1	−158.7

[a] In ppm. [b] Assuming an absolute chemical shift for the terminal hydrogens of diborane of 29.0 ppm and relative chemical shifts for $C_2B_4H_8$ and B_2H_6 from: G. Eaton and W. N. Lipscomb, "NMR Studies of Boron Hydrides and Related Compounds," W. A. Benjamin, Inc., New York, N. Y., 1969.

this choice of origin the σ_d values predict the order of resonances for H bound to B (from high to low field) to be $H_b > H_1 > H_3 > H_2$ and the experimental order is $H_b > H_1 > H_3 \approx H_2$. Of course the chemical shift differences are not accurately predicted by considering diamagnetic effects alone. It is interesting that at this choice of origin the net effect of σ_p is to shift the apical proton H_1 downfield relative to H_2 and H_3, opposite to the direction usually assumed[15] for paramagnetic effects.

The calculated σ_d values and experimental ^{11}B chemical shifts relative to boron trifluoride ethyl etherate are presented in Table IX. Again, at this choice of origin

Table IX. ^{11}B Chemical Shifts

Atom	σ_{exp}[a]	σ_d[b]
B_1	50.5	381.2
B_2	0.6	362.9
B_3	3.3	367.9

[a] In ppm relative to boron trifluoride ethyl etherate. Footnote *b*, Table VIII. [b] These values may not be directly compared to σ_{exp} because the absolute ^{11}B chemical shifts are not known.

the σ_d values correctly predict relative chemical shifts, but not exact chemical shift differences. The σ_p values cannot be calculated for boron because of the lack of absolute experimental ^{11}B chemical shifts. We again emphasize that both σ_d and σ_p are gauge dependent, although in the limit of a complete basis set their sum is not.

Reactivity

Simple static indices such as Mulliken charges and frontier orbital populations have been remarkably successful in predicting electrophilic or nucleophilic reactivity in the boron hydrides and carboranes. However, as noted in the previous paper, these indices are usually considered to be valid only if the course of a reaction is determined principally by the ground-state charge distribution and if there are no subsequent substituent rearrangements. For $C_2B_4H_8$ the Mulliken charges, inner-shell eigenvalues (Table VII) and the sum of atomic populations in the first two occupied and unoccupied orbitals (Table X) all predict that the order of

Table X. Sum of Atomic Populations in the First Two Occupied and Unoccupied Orbitals

	Occupied	Unoccupied
B_1	0.91	0.11
B_2	0.29	0.93
B_3	0.47	0.64

electrophilic substitution should be $B_1 > B_3 > B_2$ and the reverse order for nucleophilic substitution. In fact, chlorination and bromination under electrophilic conditions occur exclusively at B_3, and thus the ground-state charge distribution seemingly does not determine the course of these reactions. The experimental order of nucleophilic substitution is not known.

A closer look at the symmetry of the orbitals involved suggests a possible reason for this discrepancy. The sterically most favorable approach of an electrophile for apex substitution is clearly along the mirror plane and adjacent to B_1 and B_2. However, the highest occupied orbital of $C_2B_4H_8$ is of A'' symmetry (antisymmetric about the molecular mirror plane) and has a very large contribution from the p_y orbital on B_1 (0.47 electron). For the specified approach, overlap of an electrophile's virtual orbitals of A' symmetry (necessary for the formation of a σ bond) with the B_1 p_y orbital is zero by symmetry. Thus, the electrophile–B_1 bonding interaction should be much less than would be expected on the basis of Mulliken charges alone. The same argument holds for B_2. We therefore feel that considerable care must be exercised when using Mulliken charges to predict reactivity if specific, chemically reasonable transition states can be found in which orbital symmetries are not conducive to σ-bond formation. In such a case a complete knowledge of the carborane–electrophile potential surface may be necessary to correctly predict the position of substitution. We must point out, however, that this does *not* mean that the reaction is symmetry forbidden in the Woodward–Hoffmann sense.

It is of considerable interest to examine the reactivity predictions of B_5H_9 and B_6H_{10} in the light of the above argument, since Mulliken charges predict apical electrophilic substitution for both molecules. The highest occupied orbitals of B_5H_9 are a pair of doubly degenerate E orbitals and effective overlap with an electrophile's virtual orbital is easy to achieve. Of course experimentally electrophilic substitution does occur[16] on the apex of B_5H_9. For B_6H_{10}[11c] the highest occupied orbital is of A' symmetry, but the next orbital is A'' with a large contribution from the atomic orbitals of B_1, and we view with caution the prediction of a large electrophilic reactivity at the apex. The experimental reactivity is not known. Finally, we point out that in molecules such as B_4H_{10} and $C_2B_5H_7$ a symmetry argu-

(15) W. N. Lipscomb, "Boron Hydrides," W. A. Benjamin, New York, N. Y., 1963, p 149.

(16) T. Onak, G. B. Dunks, J. W. Searcy, and J. Spielman, *Inorg. Chem.*, **6**, 1476 (1967).

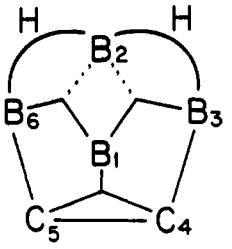

Figure 7. Localized orbitals for $C_2B_4H_8$.

ment such as the one invoked above is not straightforwardly applicable, since all boron atoms lie on a symmetry plane of the molecule and the sterically most favorable approach of an electrophile is not obvious. However, Mulliken charges correctly predict electrophilic reactivity in $C_2B_5H_7$ and the reactivity of B_4H_{10} is not known.

Localized Orbitals

A short discussion of the ER method for obtaining LMO's and general results for other boron hydrides may be found in the previous paper. We now introduce the use of a modified Taylor's (MT) method of localization and discuss the initial application of the MT method to a large polyatomic molecule.

Taylor[9f] has shown that if ψ is a determinantal wave function composed of spacial orbitals $\phi_1, \phi_2, \ldots, \phi_n$ with a self-repulsion energy J_0 and O is a unitary matrix defined in terms of a skew symmetric matrix A and a scalar parameter ϵ

$$O = I + \epsilon A + {}^1/_2\epsilon^2 A^2 + \sum_{i \geq 3} \epsilon^i A^i \qquad (1)$$

then the self-repulsion energy of the wave function $\psi' = \psi O$ is given by

$$J' = J_0 + 4\sum_{i>j}[(\phi_i\phi_i|\phi_i\phi_j) - (\phi_j\phi_j|\phi_j\phi_i)]A_{ji} + \epsilon^2 j_2 + \epsilon^3 j_3 + \ldots \qquad (2)$$

In this expansion the A_{ij} are the independent elements of the skew symmetric matrix A. Taylor defines the direction of steepest ascent by choosing $A_{ji} = {}^1/_4 \cdot ((ii|ij) - (jj|ji))$ and constructs the matrix O using the functional form

$$O = \left(I + \frac{\epsilon}{2}A\right)\left(I - \frac{\epsilon}{2}A\right)^{-1} \qquad (3)$$

correct to second order. The scalar parameter ϵ is found by calculating J_2 and solving $\partial J'/\partial\epsilon = 0$ to second order. Our modification of this procedure consists of only calculating J_1 and then numerically maximizing J' by varying ϵ. The process is then repeated until the calculation converges. By this procedure we obtain the maximum increase in J' for each MT iteration, since numerical evaluation of ϵ implicitly takes into account the higher order terms in the series expansion (eq 2) which are not calculated.

The localization was initiated with five ER iterations. At this point the gradient of the self-repulsion energy surface in the direction of steepest ascent, given by[9f]

$$|\nabla J|_{\max} = \left(\sum_{i>j}[(ii|ij) - (jj|ji)]^2\right)^{1/2}$$

was found to be 0.0024. Two MT iterations then reduced the gradient by 17% and produced an increase in J' roughly equivalent to one ER cycle; however, the two MT iterations required considerably less computation time than one ER iteration. Since the root-mean-square difference $D_{RMS} = 2|\nabla J|_{\max}/n(n-1)$ in the integrals $(\phi_i\phi_i|\phi_i\phi_j) - (\phi_j\phi_j|\phi_j\phi_i)$ was 1.05×10^{-5} au, the calculation was considered to have converged. The resultant LMO's are given in Table XI and Figure 7.

Table XI. Localized Orbitals

	Populations			Hybridization			% delocalization[a]
	B(C)	B(C,H)	B	B(C)	B(C)	B(C)	
			Inner Shells				
B_1	2.00						5.09
B_2	2.00						4.98
B_3	2.00						5.12
C_4	2.00						4.24
			B–H_t and C–H_t Orbitals				
B_1–H_1	0.92	1.09		1.43			8.81
B_2–H_2	0.95	1.06		1.45			8.64
B_3–H_3	0.92	1.09		1.56			8.61
C_4–H_4	1.04	0.98		1.82			9.80
			B–H_b–B Orbitals				
B_2–H_7–B_3	0.47	1.01	0.53	4.32		3.74	14.46
			Framework Orbitals				
B_1–B_2–B_3	0.74	0.50	0.65	3.93	2.39	6.52	21.50
B_1–B_2–B_6	0.74	0.50	0.65	3.93	2.39	6.52	20.88
B_1–C_4–C_5	0.63	0.66	0.65	2.52	18.6	18.6	14.66
B_3–C_4	0.82	1.21		2.08	1.50		15.08
B_6–C_5	0.82	1.21		2.11	1.50		15.07
C_4–C_5	1.01	1.01		1.85	1.85		17.05

[a] The % delocalizations found in ref 11 are apparently incorrect. They should be multiplied by a factor of 1.41 before comparing them with the numbers in this table.

The various components of the two-electron energy are presented in Table XII. Our experience with the MT method on $C_2B_4H_8$ and one other compound leads us to believe that in some instances it may be considerably faster than the ER procedure. A comparison of computing times for series of molecules is now being carried out. In the following section we present the details of the localization calculations and the search for a maximum on the self-repulsion energy surface.

Table XII. Components of the Two Electron Energy[a]

	Canonical	Localized
Total two electron	242.1295	242.1295
Interorbital coulomb	236.4791	215.9273
Exchange	−11.6532	−1.3772
Self repulsion	17.3035	27.5794

[a] Atomic units.

Search for a Maximum on the Self-Repulsion Energy Surface

For a converged calculation the first-order term in the series expansion (eq 2) is essentially zero, and the nature of the second-order term (the second partial derivatives) may be determined by the second-derivative test. Briefly, this test allows us to determine if the localization has converged to a true maximum or a saddle point in the self-repulsion energy. In the case of saddle point convergence, the second derivative test also gives

us the direction in the $n(n-1)/2$ dimensional space of the LMO's in which self-repulsion energy increases. Application of this test to the LMO's of $C_2B_4H_8$ showed that convergence was to a saddle point with a positive eigenvalue of +0.06. Thus there is a direction in which J increases and there must exist a new, presumably more localized, set of LMO's. A search for these orbitals was conducted along three independent lines.

I. The localized boron and carbon inner-shell orbitals were held constant and the valence orbitals were randomized. Localization of the valence orbitals by the ER procedure then yielded a set of orbitals essentially identical with the original LMO's. The possibility that the frozen inner shells prejudiced the calculation was considered and rejected because (1) analysis of the eigenvector associated with the positive eigenvalue in the second derivative test indicated that the components of the inner-shell orbitals in the direction of increasing J are very small, and (2) it has been recently shown in the localization of 1,6-$C_2B_4H_6$ that it is possible to locate maxima from a saddle point while holding inner shells constant.

II. Our second approach involves intentionally prejudicing the LMO's toward one of the previously considered structures in Figure 8. A 2×2 unitary matrix was found which mixed the two three-center BBB orbitals of Figure 7 to give a set of orbitals closely corresponding to Figure 8a. The BB single bond and inner-shell orbitals were then held constant and the remaining orbitals were subjected to one ER cycle. The orbitals remained basically the same. Next, the BBB three-center bond and the inner shells were held constant and the remaining orbitals were iterated. Again, the orbitals did not change drastically. It is especially significant that a structure such as Figure 8e did not result from this procedure. Finally, all orbitals were subjected to two ER iterations and the original saddle-point orbitals were obtained. A similar procedure was carried out starting from a set of orbitals closely resembling Figure 8c, but the same saddle-point orbitals resulted.

III. The third approach to finding a maximum in the self-repulsion energy stems from the recent development[17] of a method for obtaining a maximum in J starting from a saddle point. This method uses the eigenvector associated with the positive eigenvalue of the second derivative test and the scalar parameter ϵ to define a unitary matrix O such that the wave function $\psi' = \psi O$ has a higher self-repulsion energy than does the saddle-point wave function. ϵ must be chosen small enough that the second-order term of the Taylor series expansion, which is guaranteed to be positive by our method, dominates the higher order terms, but large enough that this term is numerically significant. Of course, since the saddle-point orbitals represent an extremum on the self-repulsion energy surface the first-order term of the series expansion vanishes. Extensive application of this method to $C_2B_4H_8$ has conclusively shown that there is no value of ϵ which satisfies the above requirements. That is, for any numerically significant value of ϵ the higher order terms will dominate the series expansion and we have effectively reached a local numerical maximum to the precision of the calculation (although in a rigorous mathematical sense the orbitals represent a saddle point). This argument does not rule out the possibility of some other *different* set of LMO's having a higher self-repulsion energy, but the arguments in I and II above lend no support to such a possibility. Thus we feel that the true maximum on the self energy surface may be quite close to the saddle point, and in another case[18] in which distinct extrema were close on a self energy surface the ER procedure consistently converged to the extremum with a lower self-repulsion energy.

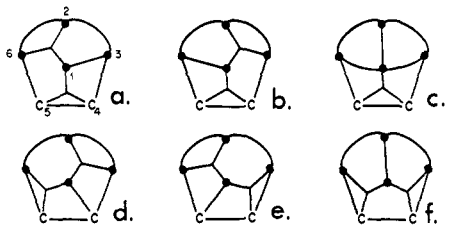

Figure 8. Other localized valence structures for $C_2B_4H_8$.

In any case, it is important to realize that our LMO's do satisfy the general *chemical* criteria usually considered desirable. They are well localized, reproducible, and to some extent transferable; compare, for example, the atomic populations of the BH and CH LMO's with other boron hydrides and carboranes. Moreover, the bond types are consistent with other localizations. These types include inner shells, B–H, C–H, C–C, C–B, C–C–B, and fractional B–B–B bonds. Also, because our LMO's transform according to the point group of the molecule we are able to meaningfully analyze the hybridization necessary for framework bonding. This result would not be true for an unsymmetrical structure. Because the true maxima probably lies quite close to the saddle-point orbitals and the important chemical criteria are satisfied by our LMO's we have chosen to analyze the bonding in terms of these orbitals.

Discussion

The localized orbitals exhibit two very interesting features. First, one atom (B_2) is participating in five bonding LMO's, including two fractional three-center BBB, two B–H–B, and a B–H_t bond. A detailed discussion of fractional bonding in this and several other molecules may be found in the previous paper; however, we emphasize here that although these LMO's do not correspond to a topologically allowed structure (see below) they do represent the best *single* valence structure which can be drawn for this molecule. Second, the hybrids on carbon involved in the C–C–B orbital are sp[19], *i.e.*, essentially 100% p orbitals. Closer examination of the atomic orbital populations indicates that the hybrids are very close to π orbitals (consider the 70° angle the hybrids make with the C–C bond, Figure 9). Thus, the prediction[4] that the two carbons make up an ethylenic system with π donation to the apex boron is completely consistent with our LMO's. The directional character (Figure 9), hybridization and per cent delocalization (Table XI) of the other LMO's are consistent with other boron hydride and carborane localizations.[11a,c]

(17) D. S. Marynick and E. Switkes, *Chem. Phys. Lett.*, **15**, 133(1972).

(18) I. R. Epstein, D. S. Marynick, and W. N. Lipscomb, submitted for publication.

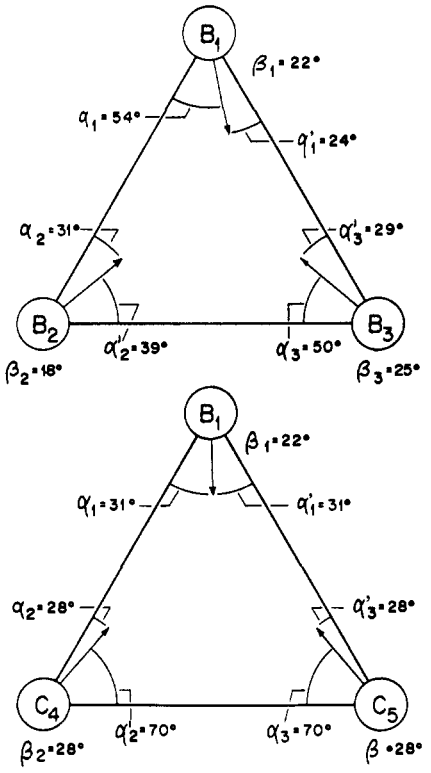

Figure 9. Directional character of the hybrids in the unique faces of the $C_2B_4H_8$ pentagonal pyramids. The out-of-plane angle of the hybrid is indicated by β.

Another interesting aspect of the valence structure of this compound lies in the application of the topological theory of the boron hydrides. If we make the usual assumption of equivalence of C to B^-, and treat the molecule according to the revised topological theory,[8] we find that there are no topologically allowed structures. This result arises from the rule that no two atoms may be connected by both a single and a three-center bond, but it is clear that when at least one of the atoms is carbon this particular rule must be relaxed. If so, all of the structures of Figure 8 except for 8c would be topologically allowed, since the revised topological theory does not presently allow open BBB three-center bonds. Finally, we again point out that the topological approach is useful only if it is possible to find linear combinations of allowed structures (with the above modification) which correctly describe the bonding. If we consider the charges and overlap populations (Table XIII) of the structures in Figure 8 we find that a simple linear combination of structures 8a, 8b, and 8f exactly reproduces the relative SCF charges and bond orders when restricted to atoms and bonds of the same type.

Table XIII. Population Analysis for Structures in Figure 8

	8a,b	8c	8d,e	8f
		Charges		
B_1	−0.33	−0.67	−0.33	−0.33
B_2	+0.33	0.00	+0.33	0.00
B_3	−0.33	0.00	−0.17	−0.17
		Overlap Populations		
B_1B_2	0.67	1.00	0.67	1.00
B_1B_3	0.83	0.50	0.67	0.67
B_2B_3	0.33	0.0	0.33	0.00
C_4B_1	0.67	0.67	0.83	0.67
C_4B_3	1.0	1.0	1.33	1.67

We conclude by pointing out two modifications of the topological theory necessary as the theory is extended to carboranes. First, new specific bonding arrangements may become allowed.[19] An example is the combination of a single bond and a central three-center bond necessary here for the CC or CB interaction of $C_2B_4H_8$. Thus a more detailed description requires topological distinctions between boron and carbon. Second, a new weighting scheme must be developed which accurately reproduces relative SCF charges and bond orders. It is our hope that SCF studies of a large number of boron hydrides and carboranes will eventually allow us to develop a consistent, reliable, and useful topological theory.

We feel that the objective localization of orbitals used here may be very informative in the less well understood structures of elemental boron, of berylides, and of other intermetallic compounds, and perhaps metals themselves. However, it may be too early to risk generalizations until localized molecular orbitals in a number of more complex molecules have been studied in detail, including $B_{10}H_{14}$ which is presently under investigation. We were surprised by the localization behavior described here for $C_2B_4H_8$. We have also found that our best locations so far in tetrahedral B_4H_4 give *unsymmetrical* BBB bonds in the faces of the B_4 tetrahedron, and are further surprised by the failure of the external B–H bonds to localize well in B_4H_4. These new results will be reported shortly.[20]

Acknowledgment. Support of this research by the Office of Naval Research and the National Institutes of Health and the award of a Predoctoral Fellowship by the National Science Foundation are gratefully acknowledged. We also thank Dr. Richard M. Stevens for use of his polyatomic SCF program.

(19) In ref 18 we will show the necessity for an open three-center BCB bond for topological description of some closed polyhedral carboranes.

(20) J. H. Hall, Jr., I. R. Epstein, and W. N. Lipscomb, to be submitted for publication.